A new experimental mouse model of water intoxication with sustained increased intracranial pressure and mild hyponatremia without side effects of antidiuretics

Bordoni, Luca; Jiménez, Eugenio Gutiérrez; Nielsen, Søren; Østergaard, Leif; Frische, Sebastian

Published in:
Society & Animals

DOI (link to publication from Publisher):
10.1538/expanim.19-0040

Publication date:
2020

Document Version
Publisher's PDF, also known as Version of record

Experimental Animals
Exp. Anim. 69(1), 92–103, 2020

Original

A new experimental mouse model of water intoxication with sustained increased intracranial pressure and mild hyponatremia without side effects of antidiuretics

Luca BORDONI[1)], Eugenio Gutiérrez JIMÉNEZ[2)], Søren NIELSEN[3)], Leif ØSTERGAARD[2,4)] and Sebastian FRISCHE[1)]

[1)]*Department of Biomedicine, Wilhelm Meyers Allé 3, Aarhus University, 8000, Aarhus, Denmark*
[2)]*Center of Functionally Integrative Neuroscience, Department of Clinical Medicine, Palle Juul-Jensens Blvd. 99, Aarhus University Hospital, 8200, Aarhus N, Denmark*
[3)]*Aalborg University, Fredrik Bajers Vej 7, 9220 Aalborg Ø, Denmark*
[4)]*Department of Neuroradiology, Nørrebrogade 44, Aarhus University Hospital, 8000, Aarhus, Denmark*

Abstract: The most used experimental mouse model of hyponatremia and elevated intracranial pressure (ICP) is intraperitoneal injection of water in combination with antidiuretics. This model of water intoxication (WI) results in extreme pathological changes and death within 1 h. To improve preclinical studies of the pathophysiology of elevated ICP, we characterized diuresis, cardiovascular parameters, blood ionogram and effects of antidiuretics in this model. We subsequently developed a new mouse model with mild hyponatremia and sustained increased ICP. To investigate the classical protocol (severe WI), C57BL/6mice were anesthetized and received an intraperitoneal injection of 20% body weight of MilliQ water with or without 0.4 $\mu g \cdot kg^{-1}$ desmopressin acetate (dDAVP). Corresponding Sham groups were also studied. In the new WI protocol (mild WI), 10% body weight of a solution containing 6.5 mM $NaHCO_3$, 1.125 mM KCl and 29.75 mM NaCl was intraperitoneally injected. By severe WI, ICP and mean arterial pressure increased until brain stem herniation occurred (23 ± 3 min after injection). The cardiovascular effects were accelerated by dDAVP. Severe WI induced a halt to urine production irrespective of the use of dDAVP. Following the new mild WI protocol, ICP also increased but was sustained at a pathologically high level without inducing herniation. Mean arterial pressure and urine production were not affected during mild WI. In conclusion, the new mild WI protocol is a superior experimental model to study the pathophysiological effects of elevated ICP induced by water intoxication.
Key words: desmopressin, hyponatremia, intracranial pressure, mouse model, water intoxication

Introduction

Hyponatremia (HN) (defined as $[Na^+]$<135–136 mM in plasma) [47] is the most common electrolytic disorder encountered in the clinical practice, with an estimated 15–30% of hospitalized patients experiencing mild HN ($[Na^+]$>130 mM) [50], and 7% developing moderate to severe HN ($[Na^+]$<126 and 116 mM, respectively) [19]. Several epidemiological studies have found an association of HN with increased mortality and longer hospitalization independently by its severity [5, 7, 17]. A crucial pathological factor determining the outcome of HN is the development of hyponatremic encephalopathies and brain edema (BE) [54]. The highest risk of cerebral sequelae is posed by severe and acute HN (<48 h) [43], which can induce osmotic brain swelling and increased intracranial pressure (ICP) leading to brain herniation and death [35]. Chronic (>48 h) and mild HN induces minor brain swelling as the brain is able to compensate for the decreased osmolarity [15] but, neverthe-

(Received 2 April 2019 / Accepted 26 August 2019 / Published online in J-STAGE 18 September 2019)
Corresponding author: S. Frische. e-mail: sfri@biomed.au.dk

less, it is associated with neurocognitive dysfunctions as impaired cognition, alertness, headaches and confusion [16, 36, 37]. Hyponatremia-related mortality is independent on its severity [7, 17] and mild HN is clinically more frequent than severe HN [50].

Very few studies have investigated whether ICP is elevated in patients with mild but acute HN, which until recently has been considered asymptomatic [9, 54]. Due to the invasive nature of current techniques, ICP monitoring is not performed in patients without a clear indication of high ICP [34]. Animal studies are limited in this regard because, with the exception of chronic HN-models of syndrome of inappropriate anti-diuretic hormone (SIADH) [13, 53], few animal models have focused on mild HN. Therefore, due to the lack of appropriate models, it is not known if elevated ICP contributes to the neurocognitive sequelae of mild HN.

The most common experimental models to study the pathophysiology of HN-induced BE and elevated ICP rely on the application of a large amount of hypo-osmolar fluid to experimental animals, a procedure commonly known as water intoxication (WI) [38]. WI has been performed on a wide range of animals: monkeys [8], dogs [8, 38, 44], rabbits [2, 10], pigs [32, 33] and rodents, both rats [3, 4, 24, 27, 30, 45, 55] and mice [1, 25, 31, 48, 52, 56, 57]. Most WI models are based on the intraperitoneal (IP) injection of large volumes of hypo-osmolar fluid (10–40%) [29] and produce severe HN characterized by extremely elevated ICP (>40 mmHg) and death [25] within 60 min. The high severity decreases the translational value since the clinical range initiating treatment of elevated ICP is well below 40 mmHg (ICP>22 mmHg and ICP<30 mmHg) [28, 42]. In addition, in current WI models, severe HN develops acutely within min from water injection [56] which further narrows the translational relevance of WI, because mild HN is far more clinically prevalent [50]. Hence, classical WI models have limited potential to investigate the most clinically relevant ranges of elevated ICP and HN.

In most of the studies, WI was coupled with antidiuretic pre-treatments as arginine vasopressin (AVP) [2–4, 10, 12, 51], pitressin [18], or the AVP analogue desmopressin acetate (dDAVP) [1, 25, 33, 52, 57]. The rationale for the use of AVP or analogue compounds in non-SIADH models [53] is to avoid an increased renal water excretion as a compensation to the decreased plasma osmolarity [18]. However, the few studies measuring urine production in WI without antidiuretics reported limited renal compensation to the water load [8, 10] and no study systemically evaluated the effect of antidiuretics in the WI model. Thus, it is an open question if the use of non-endogenous AVP or analogues results in independent side effects on top of WI-induced pathology.

Based on these premises, we defined these aims of the study:

1) to evaluate if the application of dDAVP has significant effects in the classic mouse model of severe WI (20% body weight (BW) infusion of distilled water) in terms of urine production, cardiovascular and cerebral physiology.

2) to establish a new mouse model of WI with acutely elevated ICP and mild HN, and to characterize this model in terms of cardiovascular parameters, ICP, diuresis and plasma composition.

Materials and Methods

Experimental animals

Experiments were conducted following approval from the Danish Animal Experiments Inspectorate (Permit: 2015-15-0201-00509). Male C57BL/6 mice (Taconic, Ejby, Denmark) (9–18 weeks old; BW 24–30 g (26.9 ± 1.9 g) were used in the study. Animals were housed at the Danish Neuroscience Center (DNC, Aarhus University, Aarhus, Denmark) in group cages (3–5 mice/cage) with *ad libitum* access to water and standard diet (Altromin 1320) and with a 12h:12h light-dark cycle at 21 ± 2°C and 45 ± 5% relative humidity.

Experimental protocols

The study design is summarized in Table 1. Experimental protocol 1 was designed to characterize the physiology of the mild WI model with respect to severe WI. Four mice underwent severe WI with dDAVP as described below. Seven mice were exposed to mild WI (described below).

Experimental protocol 2 was designed to evaluate the effect of dDAVP during severe WI. Four groups of 6 mice each were randomly assigned in the following groups: WI with dDAVP (WI+); WI without dDAVP (WI−); Sham with dDAVP (Sh+); Sham without dDAVP (Sh−). Severe WI was performed as described below. Animals in the WI+ group received 0.4 $\mu g \cdot kg^{-1}$ dDAVP ([1-deamino-Cys, 8-D-Arg]AVP, V1005, Sigma Aldrich, St. Louis, MO, USA), dissolved in the sterile water used for WI (volume indicated below). Animals in the Sh+ group received dDAVP 0.4 $\mu g \cdot kg^{-1}$ IP in 100 μl saline. Sh− grouped received 100 μl saline vehicle.

Surgical procedures

Surgical anesthesia was induced using 3% Isoflurane (ISO, ISO-Vet, 100%, Abbott, Chicago, IL, USA) carried

Table 1. Schematic summary of experimental protocols, animals groups, surgical procedures and data collected in this study

	Groups	Surgery	Timeline	Data
Protocol 1	Severe WI (n=4) [20 % BW − MilliQ water] Mild WI (n=7) [10% BW − 36.25 mM Na^+]	Bladder catheter Artery catheter (femoral artery) Tracheostomy (mechanical ventilation) ICP-probe insertion	1. Isoflurane: 3% induction 1.5–1.75% maintainance 2. Surgerical procedures 3. Time: -40–0 min. Baseline recording 4. Time: 0 min. WI induction 5. Time: 0–60/90 min. WI recording	MAP (and HR) ICP CPP = MAP − ICP Urine production Arterial blood gases and ions
Protocol 2	Severe WI + dDAVP (n=6) Severe WI − dDAVP (n=6) Sham + dDAVP (n=6) Sham − dDAVP (n=6)	Bladder catheter Artery catheter (femoral artery) Tracheostomy (mechanical ventilation)	1. Isoflurane: 3% induction 1.5–1.75% maintainance 2. Surgerical procedures 3. Time: -40–0 min. Baseline recording 4. Time: 0 min. WI induction 5. Time: 0–60 min. WI recording	MAP (and HR) Urine production Arterial blood gases and ions

WI, water intoxication; BW, body weight; dDAVP, desmopressin acetate; MAP, mean arterial pressure; HR, heart rate; ICP, intracranial pressure; CPP, cerebral perfusion pressure.

by a 9:1− mixture of medical air and oxygen (30% FiO_2). ISO was reduced to 1.5–1.75% for maintenance. After induction of anesthesia, mice were moved to a heating pad connected via feedback to a rectal thermometer (HB 101/2, Harvard Apparatus, Cambridge, MA, USA) to maintain body temperature at 37 ± 0.5°C. Eye ointment was applied to prevent eye dehydration. To maintain hydration status, 50 μl of saline solution (0.9% NaCl) were injected IP every hour prior to WI initiation.

All surgical procedures were performed under a dissection microscope (Olympus, SZ-TB1, Tokyo, Japan). Prior to surgery, 0.02 ml of Lidocaine (D04AB01, 10 $mg \cdot ml^{-1}$) were injected subcutaneously into all surgical sites. The following surgical procedures were performed in both experimental protocols.

a) Bladder catheterization: an abdominal incision (2 cm) was performed. Abdominal muscles were carefully trimmed and the bladder exposed. A small incision on the bladder was made and the catheter (PE50, inner diameter (id): 0.5 mm, Intramedic Clay Adams, Becton Dickinson, Franklin Lakes, USA), was carefully inserted and secured to the bladder with silk sutures. After surgical closure, urine was collected from the catheter in 75 μl non-heparinized capillary tubes and diuresis measured by recording the length of the liquid column in the tube at fixed time points.

b) Cannulation of femoral artery: A small incision (1 cm) was made in the left inguinal region and tissue was dissected until the vessels were visible. The artery was dissected from femoral vein and nerve and transiently clamped before catheter insertion to prevent back-flow. A catheter (PE10, id: 0.28 mm) filled with 5% heparinized saline (Heparin LEO, 100 $U \cdot ml^{-1}$, Leo Pharma, Ballerup, Denmark) was advanced towards abdominal aorta. The catheter was secured to the skin by silk sutures during surgical closure.

c) Tracheostomy: A PE90 catheter (id: 0.8 mm) was inserted in the trachea and immediately connected to artificial ventilation apparatus (SAR-830/P, CWE Inc., Ardmore, PA, USA). ISO administration was continued through tracheal tube.

In experimental protocol 1, an additional surgical procedure was performed to measure ICP. The head of the mouse was shaved and the left frontal bone was secured to a custom-made head frame with dental cement (GC Fuji PLUS, GC Europe, Leuven, Belgium). A circular area of ~3 mm in diameter between temporal and parietal muscle was drilled at 1,000 round per min (RPM) until intact dura was visible. An ICP transducer (Codman Microsensor, DePuy Synthes, Warsaw, IN, USA) was inserted between the skull and dura. The sensor was fixed to the skull with biocompatible, temporary dental cement (Speiko, Münster, Germany).

Physiological monitoring

Physiological data were digitally collected using a PowerLab 8/35 data acquisition device and LabChart acquisition software (ADInstruments Ltd., Oxford, UK). End-tidal pCO_2 ($EtCO_2$) was monitored by a capnograph (MicroCapStar End-Tidal CO_2 Analyser, CWE Inc.).

After synchronization, ventilation parameters were adjusted to maintain $EtCO_2$ in a range between 35–45 mmHg. Ventilation parameters were based on manufacturer instruction and previous studies [40].

Mean arterial pressure (MAP) and heart rate (HR) were monitored by a pressure transducer (BLPR2, WPI Inc., Sarasota, FL, USA) connected to the arterial catheter. Arterial pH, pCO_2, pO_2, $[Na^+]$, $[K^+]$, $[Cl^-]$, $[HCO_3^-]$, oxygen saturation of hemoglobin (sO_2) and hemoglobin concentration (ctHb) were examined on a blood gas analyzer (ABL90FLEX, Radiometer, Copenhagen, Denmark) on 70 μl blood samples.

The prolonged use of inhalation anaesthetics can induce severe respiratory suppression [49], acidosis [20], dose-dependent hypotension [14] and a higher permeability of blood brain barrier [46] in experimental mice. To minimize the interference of anaesthesia on the results from experimental animals, we defined exclusion criteria at baseline. WI was performed only if the monitored physiological parameters were within the following limits: pH (7.35–7.45) and pCO_2 (30–40 mm Hg) [20]; (sO_2>96%) [49]; MAP>70 mmHg [58]; ICP<20 mmHg; $[Na^+]$ between 135–150 mM. If the measurements felt outside these ranges, the ventilation parameters were modified and 50 μl physiological saline was given before an additional arterial blood-sample was analyzed 10 min after intervention. Adjustments could be repeated up to a maximum of 3 times before WI and, if not successful, mice were sacrificed by cervical dislocation and excluded from the data set.

Water intoxication procedures

Two procedures of water intoxication by IP injection were used. *Severe WI*: The infused solution was 20% BW of MilliQ water (4.8–6 ml) with 0.4 $\mu g \cdot kg^{-1}$ dDAVP as used in previous studies [25]. *Mild WI*: Based on a small number of pilot-studies, the composition of the infused solution was defined as: $NaHCO_3$: 6.5 mM; KCl: 1.125 mM; and NaCl: 29.75 mM, giving a total concentration of $[Na^+]$ of 36.25 mM. Injection volume of the mild-WI solution was 10% BW (2.5–3 ml).

For both severe WI and mild WI the protocol consisted of: 1) a period of baseline monitoring (40 min); 2) 2 min of IP infusion of 37°C WI solution using an automatic infusion pump (GenieTouch Syringe pump, Kent Scientific Corp., Torrington, CT, USA); 3) a post-infusion period of WI monitoring. Mice were monitored for a maximum of 1 h after severe WI and 90 min after mild WI and then sacrificed by cervical dislocation.

Statistical analysis

Graphical representation and statistical analyses were performed on GraphPad Prism version 7.0 (GraphPad Software, La Jolla, CA, USA). Significance (P-value<0.05 (α=5%)) is indicated by the exact P-value or given as follows: *:P<0.05; **:P<0.01; ***:P<0.001. Gaussian distribution and equality of variance were checked before each test. ANOVA was followed by Fisher's LSD post-hoc test (no correction for multiple comparisons). ANOVA with matching values and paired t-tests were used for the comparison of animals with their respective baseline. Unpaired t-test was used for comparisons of severe and mild WI protocols. Data are reported as mean ± SEM, unless specified elsewhere.

Results

ICP increases and peaks within 30 min in the severe WI model

In severe WI, a significant increase of ICP from baseline was detected at 7.5 ± 2.1 min after initiation of WI. ICP then dramatically increased from a mean baseline value of 8.49 ± 3.34 mmHg to a mean peak value of 84.7 ± 3.0 mmHg (P=0.0002), which occurred at 23.0 ± 2.9 min after initiation of WI (Fig. 1a). After the MAX peak, ICP rapidly dropped to a minimum mean value of 29.9 ± 6.2 mmHg.

As a consequence of the increase in ICP and despite counteracting changes in MAP (Fig. 1b), the cerebral perfusion pressure (CPP = MAP − ICP) gradually declined during the experiment (Fig. 1c). At baseline CPP was 70.9 ± 1.74 mmHg, but after 8 min a significant fall was detected (63 ± 6.2 mmHg) in parallel to the first significant increase of ICP (7.5 min). After the ICP peak, CPP was 22.4 ± 1.04 mmHg (68% decrease, P=0.00057 vs. baseline) and continued to fall until 32.0 ± 2.0 min after WI, when MAP and ICP were approximately equal (CPP = 0.9 ± 2.0 mmHg, P=0.00003 vs. baseline).

Severe WI animals developed arterial hypertension (Fig. 1b) in response to increased ICP and showed unstable HR in the time interval 20–35 min where the highest values of ICP and MAP were recorded (Fig. 1d).

Values of $EtCO_2$ were maintained in physiological ranges by mechanical ventilation to avoid respiratory acidosis (Fig. 1e). However, even with artificial ventilation, an irregular pattern of $EtCO_2$ peaks was observed at baseline, probably caused by occasional spontaneous breathing. The pattern of $EtCO_2$ peaks became more regular ~25 min after initiation of WI. If ventilation was discontinued, the mice undergoing severe WI died.

Mild WI induced a moderate and sustained increase in ICP

Following induction of mild WI, the first significant

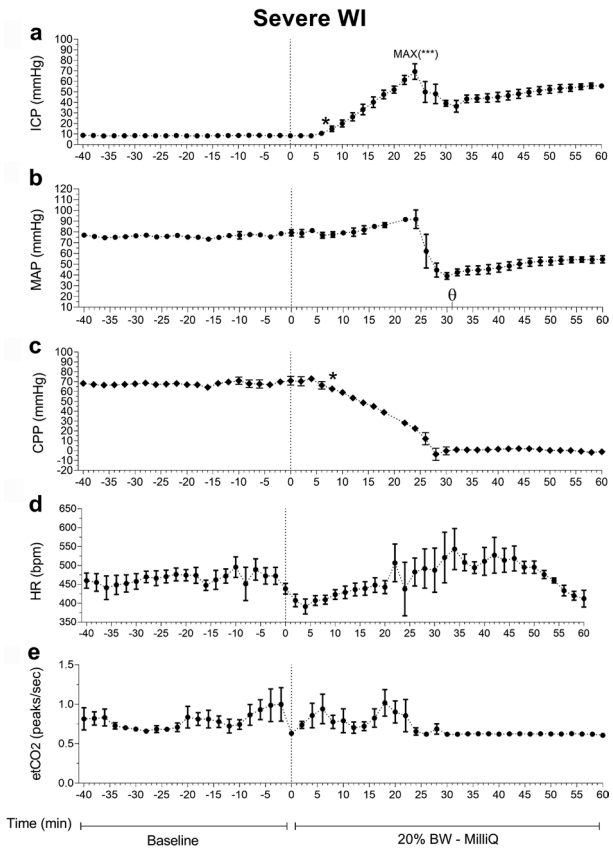

Fig. 1. Time-course of intracranial pressure (ICP), mean arterial pressure (MAP), cerebral perfusion pressure (CPP) and heart rate (HR) during severe water intoxication (WI). a, ICP; b, MAP; Θ, animal death; c, CPP; d, HR; e, end-tidal pCO_2 ($EtCO_2$) period (peaks/s). Mean ± SEM (n=4). *: first significant deviation from baseline. Time $_{(0)}$: WI initiation. MAX time of recorded ICP maximum value. Data from animals dying before the end of experiment were omitted after death. Data from experimental protocol 1. Sampling: during baseline: mean of 12 s every 2 min; after WI, mean of 5 s every 2 min.

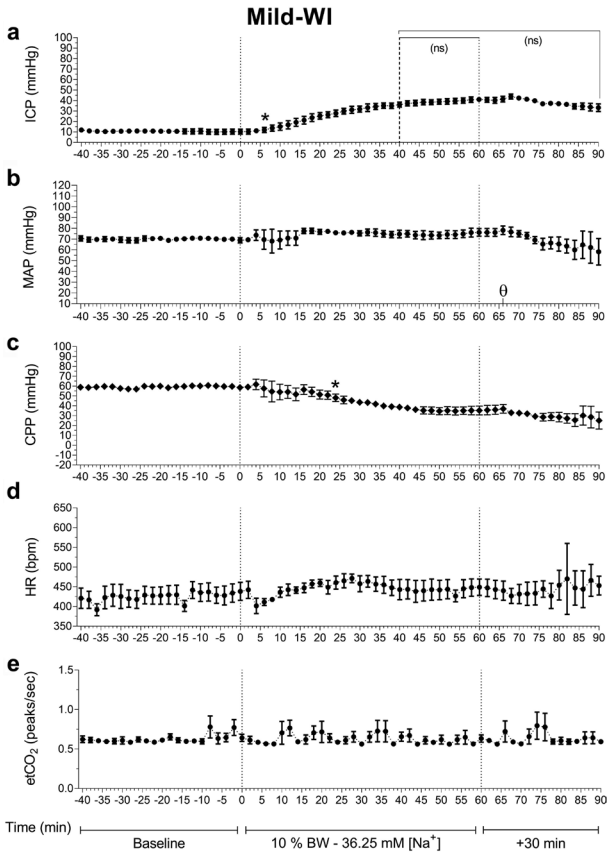

Fig. 2. Time-course of intracranial pressure (ICP), mean arterial pressure (MAP), cerebral perfusion pressure (CPP) and heart rate (HR) during mild water intoxication (WI). a, ICP; b, MAP; Θ, animal death; c, CPP; d, HR; e, end-tidal pCO_2 ($EtCO_2$) period (peaks/s). Mean ± SEM (n=4). *: first significant deviation from baseline. Time$_{(0)}$: WI initiation. Data from animals dying before the end of experiment were omitted after death. Data from experimental protocol 1. Sampling: during baseline: mean of 12 s every 2 min; after WI, mean of 5 s every 2 min.

increase in ICP from baseline was detected at 5.75 ± 0.5 min from WI initiation (ICP was 2.0 ± 1.0 mmHg higher than baseline, P=0.037) (Fig. 2a). ICP increased afterwards and 19 min after WI all animals experienced cranial hypertension (ICP>20 mmHg). The increasing trend of ICP stopped at 40 min from WI initiation, where ICP was 36.1 ± 1.2 mmHg. Between 40 to 60 min from WI (36.1 ± 1.2 vs. 41.0 ± 1.1 mmHg, respectively) the data points were statistically indistinguishable (P=0.956, one-way matched ANOVA). ICP was not different between 40 and 90 min after WI initiation (36.1 ± 1.2 mmHg vs. 33.7 ± 6.3 mmHg respectively, P=0.52). A single mouse showed a drop in ICP at 72 min from WI. MAP slightly increased from WI initiation (68.8 ± 1.3 mmHg) to 60 min after WI (76.3 ± 1.8 mmHg) (Fig. 2b), but no significant hypertensive peak was observed. The continuous increase in ICP and almost constant MAP resulted in a decrease in CPP (Fig. 2c). The first significant decrease in CPP from baseline (59.45 ± 1.35 mmHg) was detected at 24 min (45.91 ± 2.0 mmHg, P=0.046). At 60 min CPP had declined to pathological levels (35.2 ± 8.9 mmHg, 40% drop from baseline, P<0.001).

After an initial increase, HR was fairly stable 20 min after induction of mild WI (Fig. 2d). The ventilation pattern was slightly irregular for the whole experimental time after mild WI (Fig. 2e) and animals did not immediately die when artificial ventilation was temporarily discontinued (data not shown).

A direct comparison shows the increase in ICP in mice undergoing mild WI to be significantly less dramatic than in severe WI (Fig. 3a) (area under the curve (AUC): 2,481 ± 66.5 and 1731 ± 45.1 for severe WI and mild WI respectively, P<0.001). CPP was significantly more preserved and never completely abolished after mild WI (AUC: 1,330 ± 36.5 and 2,711 ± 72.2 for severe WI and mild WI respectively, P<0.001) (Fig. 3b).

 doi: 10.1538/expanim.19-0040

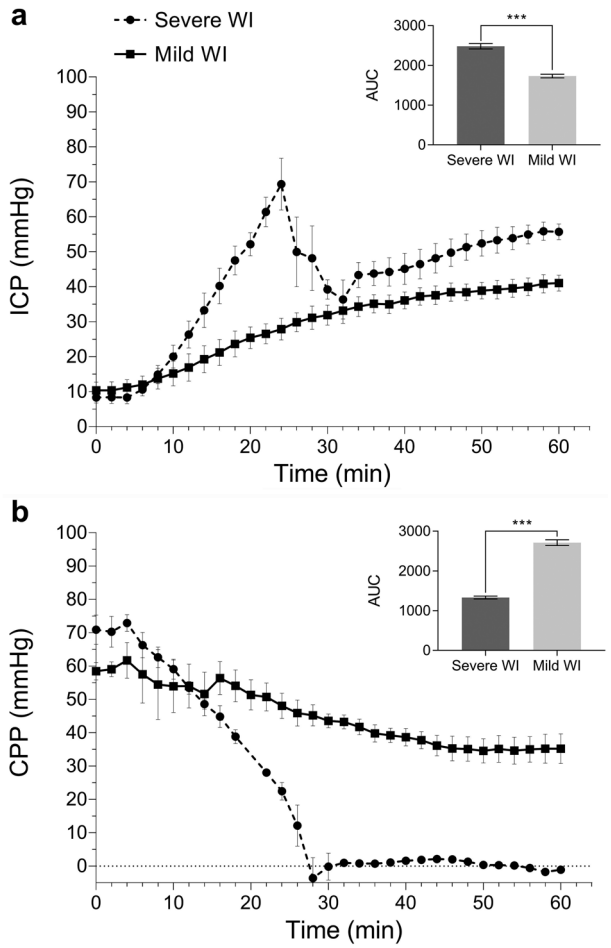

Fig. 3. Comparison of the intracranial pressure (ICP) and cerebral perfusion pressure (CPP) during severe and mild water intoxication (WI). a, ICP; b, CPP. Mean ± SEM (n=4). Severe WI (black circle, dotted line) and mild WI (black square, solid line). Data from experimental protocol 1. Statistical comparison: unpaired *t*-test of the area under the curve (AUC) of the trace for each parameter.

dDAVP accentuates changes in MAP and HR during severe WI

Similarly to Experimental protocol 1 also animals exposed to severe WI in Experimental protocol 2 experienced an increased MAP and HR after WI (Figs. 4a and c). The hypertensive peak (MAX, Fig. 4a) was recorded both in WI- (112.7 ± 24.4 mmHg, net increase: 39 ± 22.7 mmHg, P=0.019), and WI + (125.6 ± 21.5 mmHg, net increase: 52.4 ± 24 mmHg, P=0.008). The MAX peak occurred significantly earlier in the WI+ group (WI-: 25.5 ± 2.0 min, WI+: 22.6 ± 2.5 min, P=0.0339) (Fig. 4b). Shortly after the peak, MAP decreased to levels significantly below baseline in both groups (WI−: 36.0 ± 8.8 mmHg, WI+: 31.2 ± 12.5 mmHg) (net decrease: 38.0 ± 10.0 and 42.0 ± 12.0 mmHg for WI− and WI+ respectively, P=0.0013 and P=0.0016 vs. baseline) and significant hypotension was observed from ~30 min after WI initiation until the end of the experiment (mean MAP between 30–60 min after WI: 40.8 ± 11.8 in WI−, 35.9 ± 9.8 in WI+, P=0.01 and P=0.0007 vs. baseline, respectively).

A tendency towards increased HR was evident in both WI− and WI+ groups after induction of WI. Maximum HR was seen between 20 and 30 min after induction of WI (Fig. 4c). This time interval coincides with the MAX value of MAP. In this 10 min time interval, the mean HR was significantly higher in WI+ compared to WI− (P=0.0328) (Fig. 4d).

Urine flow rate is drastically reduced by severe WI irrespective of the administration of dDAVP

In Protocol 2, urine flow rate was similar at baseline in all groups but WI+, WI− and Sh+ groups showed significantly lower urine flow rates after WI (P<0.001 in all 3 groups) (Fig. 5). Administration of dDAVP induced a significantly lower urine flow rate in Sh+ animals compared to Sh− (P=0.0323), but dDAVP had no effect in WI groups since both experienced a dramatic reduction in urine production after severe WI.

In Protocol 1, urine flow rate was stable after mild WI and not significantly different between baseline period and WI (0.030 ± 0.005 vs. 0.028 ± 0.006 μl*min^{-1}*g BW^{-1}, P=0.779) (Fig. 5).

Mild WI results in sustained mild hyponatremia

Following mild WI, a significant drop in [Na^+] occurred in the first blood samples obtained after WI initiation (baseline: 149.2 ± 0.62 mM; 14.5 min: 136 ± 0.57 mM, P<0.001) (Fig. 6a), but [Na^+] was subsequently stable and mild HN was evident until the end of the experiment (133.8 ± 1.2, 133.5 ± 0.7, 135.8 ± 1.3 mM at 29, 50 and 90 min from WI, respectively). On the other hand, in severe WI mice, mild but significant HN (WI−: 130 ± 1.0 mM, WI+: 128 ± 0.28) developed within 5 min and became moderate-to-severe HN after 20 min from initiation of WI (WI−: 107.8 ± 0.9 mM, WI+: 107.6 ± 0.7 at 35 min), irrespectively of the use of dDAVP. No further changes were observed at 60 min (WI−: 103.0 ± 2.3, WI+: 105.5 ± 1.23).

Plasma [Cl^-] showed a similar pattern as [Na^+] in both severe and mild WI (Fig. 6b). Plasma [K^+] did not change, except in the late phases of severe WI where hyperkalemia was observed (Fig. 6c).

Severe, but not mild WI, induces rapid dilutional acidosis

During severe WI, a significant drop in blood pH was observed in WI groups already at 5 min (ΔpH = −0.083 ± 0.04, −0.095 ± 0.04 for WI− and +, respectively) (Table 2). Acidosis worsened after 35 min (ΔpH = −0.25

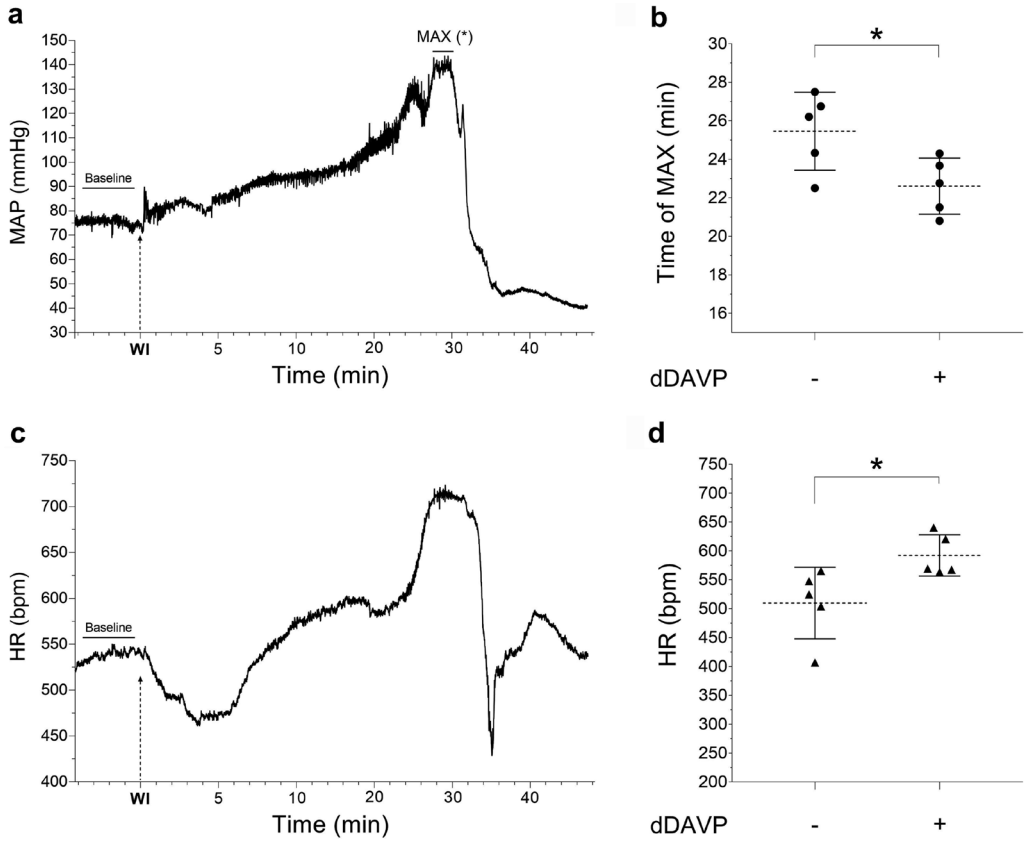

Fig. 4. Effects of desmopressin acetate (dDAVP) on MAP and heart rate (HR) during severe water intoxication (WI). a, Raw MAP trace showing the development of acute hypertension. MAX indicates maximum MAP recorded; b, Effect of dDAVP on time to MAX from WI initiation. Mean ± SEM (n=5), unpaired *t*-test; c, Representative HR trace. d, Averaged HR between $t_{(20)}$ and $t_{(30)}$ after WI of each mouse. Mean ± SEM (n=5), unpaired *t*-test. Data from experimental protocol 2.

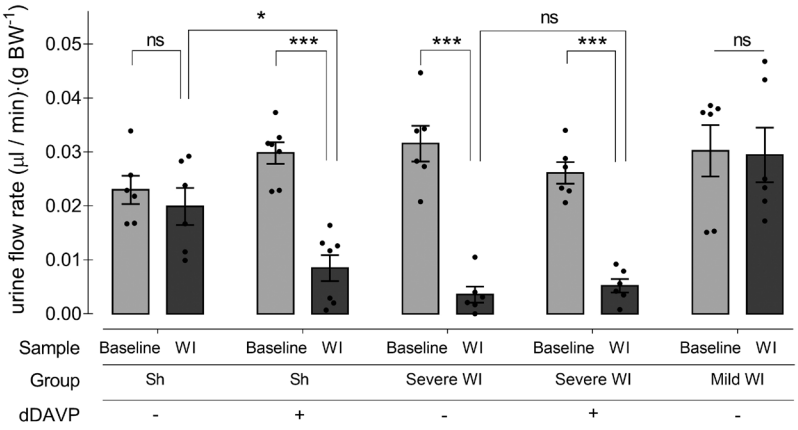

Fig. 5. Mean urine flow rate during baseline and water intoxication (WI) periods. Light Grey, Baseline; Dark Grey, WI. Mean ± SEM (n=6). Statistical comparisons: paired two-way ANOVA with Fisher's LDS post hoc test and unpaired *t*-test between WI of different groups. Data from both Experimental protocols.

and −0.28 from baseline for WI+ and −, respectively). Decreases in bicarbonate were found in both WI+ and WI− groups ($\Delta HCO_3^- = -7.0$ and −6.6 mM after 35 min, respectively) (Table 2).

In mild WI, both pH and $[HCO_3^-]$ were higher than in severe WI at similar time points (P=0.0149) (Figs. 6d and e) and acidosis occurred late in the experimental period (50 ± 4.5 min from WI). The late acidosis in mild WI animals had a respiratory origin, since $[HCO_3^-]$ did not decrease in that time period (Fig. 6e) while pCO_2

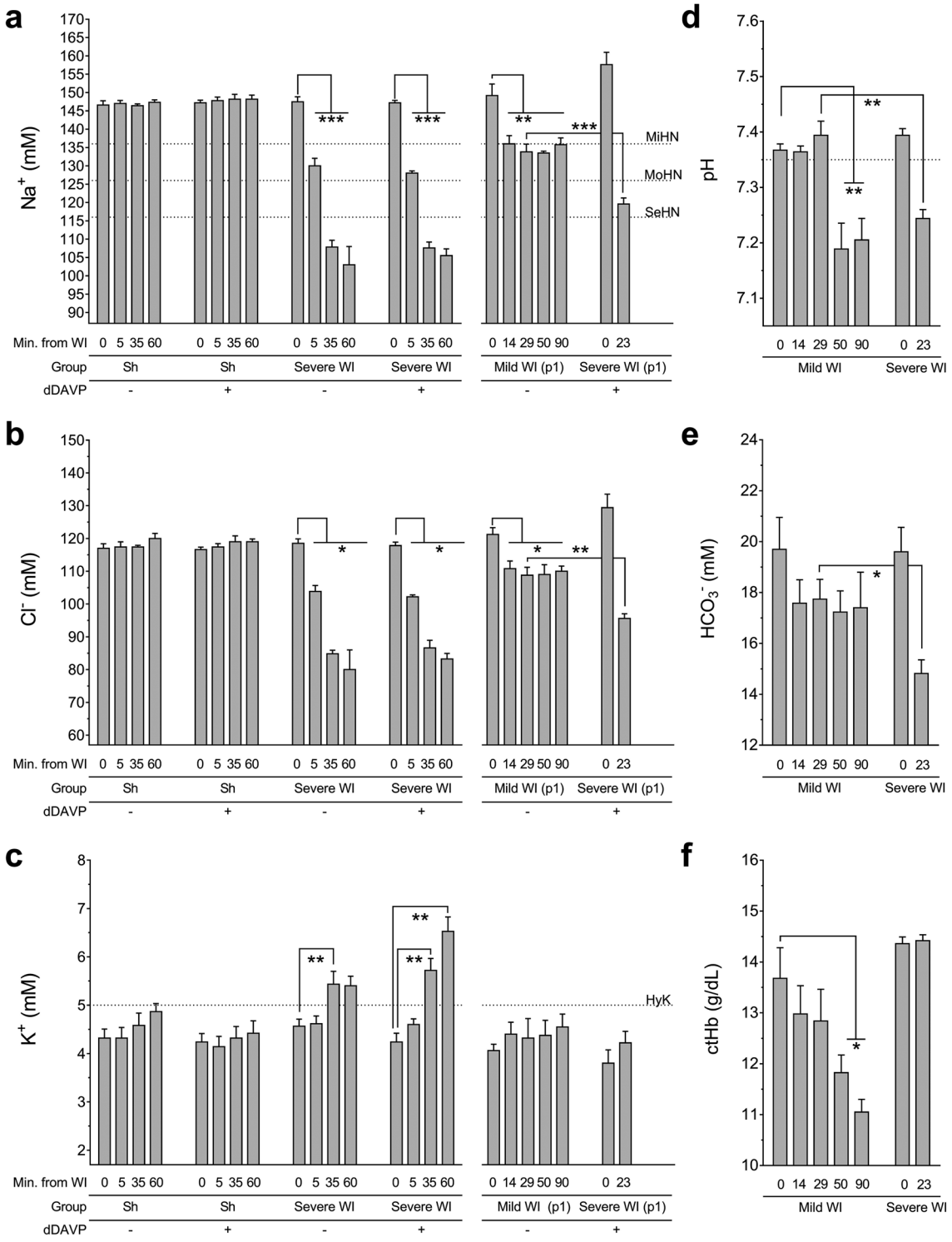

Fig. 6. Plasma ionogram and acid/base status (pH, and bicarbonate) and concentration of hemoglobin. a, sodium; b, chloride; c, potassium; d, pH; e, bicarbonate; f, hemoglobin concentration (ctHb). Statistical comparisons: paired one-way ANOVA with Fisher's LDS post hoc test (Different time points within the same group). Mean ± SEM (n=5). Data from both Experimental protocols (p1: protocol 1). Differences between the second time point (29 ± 4.4 min) of mild and severe water intoxication (WI) of Experimental protocol 1 were evaluated with unpaired *t*-test. Clinical thresholds for mild (MiHN), moderate (MoHN) and severe hyponatremia (SeHN), hyperkalemia (HyK) and acidosis are indicated by dotted horizontal lines.

increased, although not significantly (baseline: 33.2 ± 2.87 mmHg; 50 min: 43.7 ± 7.3 mmHg, P=0.107; 90 min: 47 ± 5.9 mmHg, P=0.0385).

Hemoglobin concentration is unchanged by severe WI but reduced by mild WI

Hemoglobin concentration (ctHb) was not significantly affected by severe WI or application of dDAVP

Table 2. Arterial acid/base status in severe water intoxication (WI)

Phase		Baseline	Experimental	Experimental	Experiment end
Time		0	5	35	60
pH	WI−	7.43 ± 0.04	7.35 ± 0.05**	7.18 ± 0.07**	7.2 ± 0.04**
	WI+	7.44 ± 0.04	7.34 ± 0.03*	7.15 ± 0.03***	7.06 ± 0.01**
	Sh−	7.41 ± 0.03	7.4 ± 0.04	7.42 ± 0.05	7.36 ± 0.11
	Sh+	7.43 ± 0.01	7.43 ± 0.02	7.43 ± 0.03	7.44 ± 0.04
pCO_2 (mmHg)	WI−	30 ± 1.3	30 ± 1.4	37 ± 2*	36 ± 3.1
	WI+	31 ± 2.7	34 ± 1.4	44 ± 3.9**	51 ± 6***
	Sh−	33 ± 1.1	34 ± 1.1	31 ± 1.5	33 ± 2.5
	Sh+	34 ± 1.5	33 ± 1.1	31 ± 0.5	30 ± 1.3
HCO_3^- (mM)	WI−	20.7 ± 0.6	17.2 ± 0.7***	14.1 ± 0.3***	12.4 ± 0.6***
	WI+	21.6 ± 0.9	18.8 ± 0.5**	14.6 ± 0.4***	13.3 ± 0.9***
	Sh−	21.6 ± 0.5	22 ± 0.5	21 ± 0.6	19.4 ± 0.7
	Sh+	23.3 ± 0.7	22.5 ± 0.9	21.5 ± 0.6	21.4 ± 0.4
ctHb (g/dL)	WI−	13.84 ± 0.25	13.74 ± 0.38	13.34 ± 0.42	13.3 ± 0.44
	WI+	13.32 ± 0.23	13.1 ± 0.18	12.56 ± 0.18	12.4 ± 0.28
	Sh−	13.8 ± 0.13	14.13 ± 0.12	13.93 ± 0.3	13.05 ± 0.25
	Sh+	13.14 ± 0.59	13.32 ± 0.45	13.5 ± 0.35	13.3 ± 0.3

Arterial blood acid/base status (pH, pCO_2, bicarbonate), and concentration of hemoglobin (ct[Hb]) in Experimental protocol 2. Mean ± SEM (n=5). Statistical comparisons: paired one-way ANOVA within the same group followed by Fisher's LDS multiple comparisons against baseline (time=0). *P<0.05, **P<0.01, ***P<0.001.

(Table 2 and Fig. 6f). Interestingly, a small, yet significant fall in ctHb was seen in the late phase of the mild WI experimental group (Fig. 6f).

Discussion

The time course of ICP during severe WI reflects a rapid accumulation of intracranial water due to hyponatremia/hyposmolarity followed by herniation. Despite concomitant increase in MAP during WI, CPP is extremely low 30 min after initiation of WI, and the mouse is only alive due to artificial ventilation. dDAVP induced no changes in the overall outcome, but slightly affected the time-course of changes in MAP, ICP and HR. Surprisingly, urine production was abruptly halted after severe WI even without administration of dDAVP. This finding is consistent with the sparse data in the literature on urine production during WI-induced BE [8, 10], but contrasts the assumption underlying the general use of dDAVP in this model: to block renal adaptation. Despite the abundant use of the model, the pathophysiology of the severe WI model is not fully understood, especially with respect to renal and cardiovascular changes.

The model of mild WI also showed the aimed pathophysiological changes (mild hyponatremia and elevated ICP), but did not show the complete respiratory depression, which was seen in all animals undergoing severe WI between 20 and 25 min from WI, and which is a sign of permanent damage in the respiratory center in the medulla oblongata [35]. Such damage can also result in an increased MAP [6], which was simultaneously observed prior to $EtCO_2$ peak homogenization in severe WI. Mild WI also did not result in abrupt halt of urine production, and as the mild WI model did not involve use of dDAVP, unwanted side effects from this drug are also avoided. The mild WI model may thus allow studies of renal compensation to sustained elevated ICP and sudden changes in brain osmolarity, such as changes in ion excretion or the osmopressor response [26]. Lastly, mild WI induced only acute and mild hyponatremia, which has been far less studied in animal models and, in its chronic manifestation, is associated with symptoms of neurocognitive and neurovascular impairments [9, 36, 37].

Injection of dDAVP affects cardiovascular parameters during severe WI

With dDAVP, herniation occurred slightly, but significantly, earlier, and the severe WI group treated with dDAVP had significantly higher HR when herniating. Since dDAVP had no effect on diuresis, the cardiovascular changes induced by dDAVP must be ascribed to other mechanisms than inhibition of renal water excretion.

The cardiovascular effects of dDAVP may be mediated by V1b-receptors, which dDAVP is known to activate besides their pharmacological main target: V2-receptors [39]. V1b-receptors are (among other places) found in the anterior pituitary, where they influence ACTH release, and in chromaffin cells of the adrenal

medulla, where they may control release of catecholamines, which in turn would stimulate HR and MAP [23]. Since the affinity of dDAVP towards V2-receptors is about 4-fold that of AVP [41] dDAVP may also induce its effect on cardiovascular parameters by displacement of AVP from V2-receptors. In turn, displaced AVP could activate vascular V1a receptors.

In conclusion, the results do not support the use of dDAVP in the animal model of BE induced by WI, since significant effects of the drug are observed in cardiovascular parameters rather than in reduction of urine production, which has been the main rationale for the use of dDAVP in previous studies [18]. This being said, endogenous AVP may likely play a role during BE [22]. A recent systematic review demonstrated not only that elevated ICP induces release of ADH, but also that this triggering mechanism can override the effect of plasma osmolarity on ADH [21]. Therefore, release of ADH can be promoted even in situation of plasma dilution if the brain effective circulatory volume is reduced of more than 5–10% [6] due to increased ICP. In the WI models explored in this study, ADH secretion and the consequent paradoxical reduction in renal water excretion could thus be seen as part of a physiological response to increase CPP by vasoconstriction resulting in increased MAP.

Severe WI induces hypo- or euvolemic HN, while mild WI induces sign of hypervolemia

In severe WI, the main ions in plasma ($[Na^+]$ and $[Cl^-]$) are diluted either due to expansion of plasma and ECF volume after WI (hypervolemic HN) or loss of ions from plasma circulation into the injected water in the abdominal cavity or by a combination of these two mechanisms.

In the first and third cases, ctHb would be reduced, whereas in the second case ctHb would be unchanged. In severe WI, no change in ctHb was seen in both protocols. As urine was not produced, we can exclude a renal mechanism influencing plasma ion composition, so net movement of ions into the hypo-osmolar abdominal fluid seems the dominating process leading to hypo-osmolality in the severe WI model. A study in pigs also found WI to induce hypovolemic HN by ion redistribution from ECF into the peritoneal fluid [32]. In conclusion, the severe WI procedure in mice induces euvolemic, or possibly hypovolemic HN.

The reductions in plasma ion concentrations were much smaller in mild WI than in severe WI. Mild WI animals showed a decrease in ctHb after 50 min, which indicates plasma volume expansion. Net movement of water from the injected solution to the blood thus takes place, although some ions probably also leaves plasma towards the IP fluid. As diuresis is unchanged, the water load may thus be gradually excreted by the kidneys as it enters the blood. The pathophysiological mechanisms for the apparent inability of water to pass the peritoneal membrane if injected as distilled water are unclear.

Mild WI is a new model with mild HN and sustained elevated ICP

Mild WI animals experienced a persistent state of mild HN throughout the whole experiment (until 90 min from WI) and a persistent elevated ICP (higher than 20 mmHg). The first time point in which ICP increased from baseline was not different from the severe WI model, but both the rate and the magnitude of the increase in ICP were lower following mild WI (~10-fold increase in 20 min in severe WI vs. ~6-fold increase in 40 min in mild WI). ICP fluctuated between 20–40 mmHg for most of the experimental period without a concomitant increase in MAP. As a result, CPP was stable around 60 mmHg for the first 20 min from WI, but afterwards gradually dropped to 40–45 mmHg, which in adult TBI patients is considered an indicator of potential cerebral ischemia [35]. The new model of mild WI thus enables studies in the mouse of the clinically relevant pathophysiology of elevated ICP and reduced CPP in the absence of side effects (loss of spontaneous respiration, drastic increase in MAP, decreased urine production, hyperkalemia) generated by the severe WI model.

The mild WI mouse model is therefore more useful to characterize the effect of persistently elevated ICP and the efficacy of ICP-reducing agents. The short duration of the severe model hampers the use of hard endpoints (e.g. survival) in studies of pharmacological intervention of elevated ICP, since the mice may die even before the test substances are cleared from circulation [11]. In future investigations, the mouse model of mild WI could be used for even longer studies than 90 min and may even, as the severe model has been [25], be performed without anesthesia to quantify neurological functionality and vascular cerebral effects during elevations of ICP. Due to the absence of good treatments, mild elevation of ICP is clinically often treated conservatively. The mild WI mouse model can be used to investigate new treatment options for this patient group.

Conflict of Interest

The authors have no conflicts of interest to disclose.

Acknowledgments

This study was supported by the following grant:

Aquaporins: roles in pathogenesis and treatment of hyponatremia, from the Danish Medical Research Council (id: 4004-00504). Further financial support was obtained thanks to the MEMBRANES (Aarhus University), the Faculty of Health at Aarhus University, Korningfonden and Lægeforeningen (2017-1064/102 KBN)

The authors thanks Susanne Smith Christensen (CFIN) and Stine Ledet Methmann for expert technical support and animal husbandry during the experimental work.

References

1. Amiry-Moghaddam, M., Xue, R., Haug, F.M., Neely, J.D., Bhardwaj, A., Agre, P., Adams, M.E., Froehner, S.C., Mori, S. and Ottersen, O.P. 2004. Alpha-syntrophin deletion removes the perivascular but not endothelial pool of aquaporin-4 at the blood-brain barrier and delays the development of brain edema in an experimental model of acute hyponatremia. *FASEB J.* 18: 542–544. [Medline] [CrossRef]
2. Arieff, A.I., Llach, F. and Massry, S.G. 1976. Neurological manifestations and morbidity of hyponatremia: correlation with brain water and electrolytes. *Medicine (Baltimore)* 55: 121–129. [Medline] [CrossRef]
3. Arieff, A.I., Kozniewska, E., Roberts, T.P.L., Vexler, Z.S., Ayus, J.C. and Kucharczyk, J. 1995. Age, gender, and vasopressin affect survival and brain adaptation in rats with metabolic encephalopathy. *Am. J. Physiol.* 268: R1143–R1152. [Medline]
4. Ayus, J.C., Krothapalli, R.K. and Armstrong, D.L. 1985. Rapid correction of severe hyponatremia in the rat: histopathological changes in the brain. *Am. J. Physiol.* 248: F711–F719. [Medline]
5. Balling, L., Gustafsson, F., Goetze, J.P., Dalsgaard, M., Nielsen, H., Boesgaard, S., Bay, M., Kirk, V., Nielsen, O.W., Køber, L. and Iversen, K. 2015. Hyponatraemia at hospital admission is a predictor of overall mortality. *Intern. Med. J.* 45: 195–202. [Medline] [CrossRef]
6. Boron, W. and Boulpaep, E. 2012. Medical Physiology, 2nd ed., Saunders, Philadelphia.
7. Corona, G., Giuliani, C., Parenti, G., Norello, D., Verbalis, J.G., Forti, G., Maggi, M. and Peri, A. 2013. Moderate hyponatremia is associated with increased risk of mortality: evidence from a meta-analysis. *PLoS One* 8: e80451. [Medline] [CrossRef]
8. Darrow, D.C. and Yannet, H. 1935. The changes in the distribution of body water accompanying increase and decrease in extracellular electrolyte. *J. Clin. Invest.* 14: 266–275. [Medline] [CrossRef]
9. Decaux, G. 2006. Is asymptomatic hyponatremia really asymptomatic? *Am. J. Med.* 119:(Suppl 1): S79–S82. [Medline] [CrossRef]
10. Dodge, P.R., Crawford, J.D. and Probst, T.H. 1960. Studies in experimental water intoxication. *Arch. Neurol.* 3: 513–529. [Medline] [CrossRef]
11. Farr, G.W., Hall, C.H., Farr, S.M., Wade, R., Detzel, J.M., Adams, A.G., Buch, J.M., Beahm, D.L., Flask, C.A., Xu, K., LaManna, J.C., McGuirk, P.R., Boron, W.F. and Pelletier, M.F. 2019. Functionalized phenylbenzamides inhibit aquaporin-4 reducing cerebral edema and improving outcome in two models of CNS injury. *Neuroscience* 404: 484–498. [Medline] [CrossRef]
12. Fraser, C.L., Kucharczyk, J., Arieff, A.I., Rollin, C., Sarnacki, P. and Norman, D. 1989. Sex differences result in increased morbidity from hyponatremia in female rats. *Am. J. Physiol.* 256: R880–R885. [Medline]
13. Fujisawa, H., Sugimura, Y., Takagi, H., Mizoguchi, H., Takeuchi, H., Izumida, H., Nakashima, K., Ochiai, H., Takeuchi, S., Kiyota, A., Fukumoto, K., Iwama, S., Takagishi, Y., Hayashi, Y., Arima, H., Komatsu, Y., Murata, Y. and Oiso, Y. 2016. Chronic hyponatremia causes neurologic and psychologic impairments. *J. Am. Soc. Nephrol.* 27: 766–780. [Medline] [CrossRef]
14. Gargiulo, S., Greco, A., Gramanzini, M., Esposito, S., Affuso, A., Brunetti, A. and Vesce, G. 2012. Mice anesthesia, analgesia, and care, Part I: anesthetic considerations in preclinical research. *ILAR J.* 53: E55–E69. [Medline] [CrossRef]
15. Gullans, S.R. and Verbalis, J.G. 1993. Control of brain volume during hyperosmolar and hypoosmolar conditions. *Annu. Rev. Med.* 44: 289–301. [Medline] [CrossRef]
16. Gunathilake, R., Oldmeadow, C., McEvoy, M., Kelly, B., Inder, K., Schofield, P. and Attia, J. 2013. Mild hyponatremia is associated with impaired cognition and falls in community-dwelling older persons. *J. Am. Geriatr. Soc.* 61: 1838–1839. [Medline] [CrossRef]
17. Holland-Bill, L., Christiansen, C.F., Heide-Jørgensen, U., Ulrichsen, S.P., Ring, T., Jørgensen, J.O. and Sørensen, H.T. 2015. Hyponatremia and mortality risk: a Danish cohort study of 279508 acutely hospitalized patients. *Eur. J. Endocrinol.* 173: 71–81. [Medline] [CrossRef]
18. Holliday, M.A., Kalayci, M.N. and Harrah, J. 1968. Factors that limit brain volume changes in response to acute and sustained hyper- and hyponatremia. *J. Clin. Invest.* 47: 1916–1928. [Medline] [CrossRef]
19. Hoorn, E.J., Lindemans, J. and Zietse, R. 2006. Development of severe hyponatraemia in hospitalized patients: treatment-related risk factors and inadequate management. *Nephrol. Dial. Transplant.* 21: 70–76. [Medline] [CrossRef]
20. Iversen, N.K., Malte, H., Baatrup, E. and Wang, T. 2012. The normal acid-base status of mice. *Respir. Physiol. Neurobiol.* 180: 252–257. [Medline] [CrossRef]
21. Keller, W.J. and Mullaj, E. 2018. Antidiuretic hormone release associated with increased intracranial pressure independent of plasma osmolality. *Brain Behav.* 8: e01005. [Medline] [CrossRef]
22. Kleindienst, A., Hannon, M.J., Buchfelder, M. and Verbalis, J.G. 2016. Hyponatremia in neurotrauma: the role of vasopressin. *J. Neurotrauma* 33: 615–624. [Medline] [CrossRef]
23. Koshimizu, T.A., Nakamura, K., Egashira, N., Hiroyama, M., Nonoguchi, H. and Tanoue, A. 2012. Vasopressin V1a and V1b receptors: from molecules to physiological systems. *Physiol. Rev.* 92: 1813–1864. [Medline] [CrossRef]
24. Kozler, P., Riljak, V. and Pokorný, J. 2013. Both water intoxication and osmotic BBB disruption increase brain water content in rats. *Physiol. Res.* 62:(Suppl 1): S75–S80. [Medline]
25. Manley, G.T., Fujimura, M., Ma, T., Noshita, N., Filiz, F., Bollen, A.W., Chan, P. and Verkman, A.S. 2000. Aquaporin-4 deletion in mice reduces brain edema after acute water intoxication and ischemic stroke. *Nat. Med.* 6: 159–163. [Medline] [CrossRef]
26. May, M. and Jordan, J. 2011. The osmopressor response to water drinking. *Am. J. Physiol. Regul. Integr. Comp. Physiol.* 300: R40–R46. [Medline] [CrossRef]
27. Melton, J.E. and Nattie, E.E. 1983. Brain and CSF water and ions during dilutional and isosmotic hyponatremia in the rat. *Am. J. Physiol.* 244: R724–R732. [Medline]
28. Meyfroidt, G. and Citerio, G. 2017. Letter: guidelines for the management of severe traumatic brain injury, fourth edition. *Neurosurgery.* 81: E1.
29. Michinaga, S. and Koyama, Y. 2015. Pathogenesis of brain edema and investigation into anti-edema drugs. *Int. J. Mol. Sci.* 16: 9949–9975. [Medline] [CrossRef]
30. Nagelhus, E.A., Lehmann, A. and Ottersen, O.P. 1996. Neuronal and glial handling of glutamate and glutamine during hypoosmotic stress: a biochemical and quantitative immunocytochemical analysis using the rat cerebellum as a model. *Neuroscience* 72: 743–755. [Medline] [CrossRef]

31. Nase, G., Helm, P.J., Enger, R. and Ottersen, O.P. 2008. Water entry into astrocytes during brain edema formation. *Glia* 56: 895–902. [Medline] [CrossRef]
32. Overgaard-Steensen, C., Stødkilde-Jørgensen, H., Larsson, A., Tønnesen, E., Frøkiaer, J. and Ring, T. 2016. The frequently used intraperitoneal hyponatraemia model induces hypovolaemic hyponatraemia with possible model-dependent brain sodium loss. *Exp. Physiol.* 101: 932–945. [Medline] [CrossRef]
33. Overgaard-Steensen, C., Stødkilde-Jørgensen, H., Larsson, A., Broch-Lips, M., Tønnesen, E., Frøkiaer, J. and Ring, T. 2010. Regional differences in osmotic behavior in brain during acute hyponatremia: an in vivo MRI-study of brain and skeletal muscle in pigs. *Am. J. Physiol. Regul. Integr. Comp. Physiol.* 299: R521–R532. [Medline] [CrossRef]
34. Pedersen, S.H., Lilja-Cyron, A., Andresen, M. and Juhler, M. 2018. The relationship between intracranial pressure and age-chasing age-related reference values. *World Neurosurg.* 110: e119–e123. [Medline] [CrossRef]
35. Pinto, V.L., Tadi, P. and Adeyinka, A. 2019. Increased intracranial pressure. *In*: StatPearls, StatPearls Publishing, Treasure Island. https://www.ncbi.nlm.nih.gov/books/NBK482119/
36. Refardt, J., Kling, B., Krausert, K., Fassnacht, M., von Felten, S., Christ-Crain, M. and Fenske, W. 2018. Impact of chronic hyponatremia on neurocognitive and neuromuscular function. *Eur. J. Clin. Invest.* 48: e13022. [Medline] [CrossRef]
37. Renneboog, B., Musch, W., Vandemergel, X., Manto, M.U. and Decaux, G. 2006. Mild chronic hyponatremia is associated with falls, unsteadiness, and attention deficits. *Am. J. Med.* 119: 71.e1–71.e8. [Medline] [CrossRef]
38. Rowntree, L.G. 1926. The effects on mammals of the administration of excessive quantities of water. *J. Pharmacol. Exp. Ther.* 29: 135–159.
39. Saito, M., Tahara, A. and Sugimoto, T. 1997. 1-desamino-8-D-arginine vasopressin (DDAVP) as an agonist on V1b vasopressin receptor. *Biochem. Pharmacol.* 53: 1711–1717. [Medline] [CrossRef]
40. Schwarte, L.A., Zuurbier, C.J. and Ince, C. 2000. Mechanical ventilation of mice. *Basic Res. Cardiol.* 95: 510–520. [Medline] [CrossRef]
41. Ślusarz, M.J., Ślusarz, R. and Ciarkowski, J. 2006. Investigation of mechanism of desmopressin binding in vasopressin V2 receptor versus vasopressin V1a and oxytocin receptors: molecular dynamics simulation of the agonist-bound state in the membrane-aqueous system. *Biopolymers* 81: 321–338. [Medline] [CrossRef]
42. Sorrentino, E., Diedler, J., Kasprowicz, M., Budohoski, K.P., Haubrich, C., Smielewski, P., Outtrim, J.G., Manktelow, A., Hutchinson, P.J., Pickard, J.D., Menon, D.K. and Czosnyka, M. 2012. Critical thresholds for cerebrovascular reactivity after traumatic brain injury. *Neurocrit. Care* 16: 258–266. [Medline] [CrossRef]
43. Sterns, R.H. and Silver, S.M. 2016. Complications and management of hyponatremia. *Curr. Opin. Nephrol. Hypertens.* 25: 114–119. [Medline] [CrossRef]
44. Swingle, W.W., Parkins, W.M., Taylor, A.R. and Hays, H.W. 1937. A Study of Water Intoxication in the Intact and Adrenalectomized Dog and the Influence of Adrenal Cortical Hormone Upon Fluid and Electrolyte Distribution. *Am. J. Physiol.* 119: 557–566. [CrossRef]
45. Swinyard, E.A. 1949. Effect of extracellular electrolyte depletion on brain electrolyte pattern and electroshock seizure threshold. *Am. J. Physiol.* 156: 163–169. [Medline] [CrossRef]
46. Thal, S.C., Luh, C., Schaible, E.V., Timaru-Kast, R., Hedrich, J., Luhmann, H.J., Engelhard, K. and Zehendner, C.M. 2012. Volatile anesthetics influence blood-brain barrier integrity by modulation of tight junction protein expression in traumatic brain injury. *PLoS One* 7: e50752. [Medline] [CrossRef]
47. Thompson, C., and Hoorn, E.J. 2012. Hyponatraemia: an overview of frequency, clinical presentation and complications. *Best Pract. Res. Clin. Endocrinol. Metab.* 26:(Suppl 1): S1–S6. [Medline] [CrossRef]
48. Thrane, A.S., Rappold, P.M., Fujita, T., Torres, A., Bekar, L.K., Takano, T., Peng, W., Wang, F., Rangroo Thrane, V., Enger, R., Haj-Yasein, N.N., Skare, Ø., Holen, T., Klungland, A., Ottersen, O.P., Nedergaard, M. and Nagelhus, E.A. 2011. Critical role of aquaporin-4 (AQP4) in astrocytic Ca2+ signaling events elicited by cerebral edema. *Proc. Natl. Acad. Sci. USA* 108: 846–851. [Medline] [CrossRef]
49. Tsukamoto, A., Serizawa, K., Sato, R., Yamazaki, J. and Inomata, T. 2015. Vital signs monitoring during injectable and inhalant anesthesia in mice. *Exp. Anim.* 64: 57–64. [Medline] [CrossRef]
50. Upadhyay, A., Jaber, B.L. and Madias, N.E. 2009. Epidemiology of hyponatremia. *Semin. Nephrol.* 29: 227–238. [Medline] [CrossRef]
51. Vajda, Z., Pedersen, M., Dóczi, T., Sulyok, E., Stødkilde-Jørgensen, H., Frøkiaer, J. and Nielsen, S. 2001. Effects of centrally administered arginine vasopressin and atrial natriuretic peptide on the development of brain edema in hyponatremic rats. *Neurosurgery* 49: 697–704, discussion 704–705. [Medline]
52. Vajda, Z., Pedersen, M., Füchtbauer, E.M., Wertz, K., Stødkilde-Jørgensen, H., Sulyok, E., Dóczi, T., Neely, J.D., Agre, P., Frøkiaer, J. and Nielsen, S. 2002. Delayed onset of brain edema and mislocalization of aquaporin-4 in dystrophin-null transgenic mice. *Proc. Natl. Acad. Sci. USA* 99: 13131–13136. [Medline] [CrossRef]
53. Verbalis, J.G. 1984. An experimental model of syndrome of inappropriate antidiuretic hormone secretion in the rat. *Am. J. Physiol.* 247: E540–E553. [Medline]
54. Verbalis, J.G., Goldsmith, S.R., Greenberg, A., Korzelius, C., Schrier, R.W., Sterns, R.H. and Thompson, C.J. 2013. Diagnosis, evaluation, and treatment of hyponatremia: expert panel recommendations. *Am. J. Med.* 126:(Suppl 1): S1–S42. [Medline] [CrossRef]
55. Woodbury, D.M. 1956. Effect of acute hyponatremia on distribution of water and electrolytes in various tissues of the rat. *Am. J. Physiol.* 185: 281–286. [Medline] [CrossRef]
56. Yang, B., Zador, Z. and Verkman, A.S. 2008. Glial cell aquaporin-4 overexpression in transgenic mice accelerates cytotoxic brain swelling. *J. Biol. Chem.* 283: 15280–15286. [Medline] [CrossRef]
57. Yeung, P.K., Lo, A.C., Leung, J.W., Chung, S.S. and Chung, S.K. 2009. Targeted overexpression of endothelin-1 in astrocytes leads to more severe cytotoxic brain edema and higher mortality. *J. Cereb. Blood Flow Metab.* 29: 1891–1902. [Medline] [CrossRef]
58. Zhao, X., Ho, D., Gao, S., Hong, C., Vatner, D.E. and Vatner, S.F. 2011. Arterial pressure monitoring in mice. *Curr. Protoc. Mouse Biol.* 1: 105–122. [Medline]